Defense Technical Information Center Compilation Part Notice

ADP012237

TITLE: Investigating Catalytic Properties of Composite Nanoparticle Assemblies

DISTRIBUTION: Approved for public release, distribution unlimited

This paper is part of the following report:

TITLE: Nanophase and Nanocomposite Materials IV held in Boston, Massachusetts on November 26-29, 2001

To order the complete compilation report, use: ADA401575

The following component part numbers comprise the compilation report:
ADP012174 thru ADP012259

Mat. Res. Soc. Symp. Proc. Vol. 703 © 2002 Materials Research Society V10.6

Investigating Catalytic Properties of Composite Nanoparticle Assemblies

M.M. MAYE, J. LUO, Y. LOU, N. K. LY, W.-B. CHAN, E. PHILLIP,
M. HEPEL[a], C.J. ZHONG*
Department of Chemistry, State University of New York at Binghamton, Binghamton, NY 13902. [(a)] Department of Chemistry, State University of New York at Potsdam, Potsdam, NY 13676. [(*)] cjzhong@binghmaton.edu

ABSTRACT

We present herein recent findings of an investigation of catalyst assembly and activation using metallic nanoparticles encapsulated with organic monolayers. Gold nanocrystals (2~5 nm) encapsulated with thiolate monolayers assembled on electrode surfaces, were found to be catalytically active towards electrooxidation of CO and MeOH upon activation. The activation involved partial removal of the encapsulating thiolates and the formation of surface oxygenated species. A polymeric film was also used as a substrate for the assembly of the nanoparticle catalysts. When the polymer matrix was doped with small amounts of Pt, a remarkable catalytic activity was observed. These catalysts were characterized utilizing cyclic voltammetry and atomic force microscopy.

INTRODUCTION

The pioneer work of two-phase synthesis of gold nanoparticles with a few nm core size stabilized by alkanethiolate monolayers has led to increasing research and development interest in the field of composite nanomaterials [1]. The possibility of further processing of these particles into highly monodispersed, larger sized, and stable nanoparticles has enabled the ability to probe size-dependent reactivity, as recently demonstrated in our laboratory [2]. These nanoparticles can be effectively linked to form thin films using molecular crosslinking agents. There are several routes reported for crosslinking. One involves a stepwise "layer-by-layer" assembly method [3], and another involves one step "exchange-crosslinking-precipitation" route developed recently in our laboratory [4]. The nanostructured thin films have potential applications in microelectronics, optics, biomimetics, molecular recognition, drug delivery, chemical and environmental sensing, and catalysis [5,6,7].

Gold is traditionally considered as catalytically inert. The recent finding by Haruta and co-workers [8] demonstrated that the catalytic ability for gold increases as the size is reduced to nanometer scales [9]. Gold nanoparticles supported on oxides show high catalytic activity to CO oxidation. Although the idea of using small sized particles as catalysts has been known for a long time, problems faced when using bare nanoparticles include aggregation, short life times, and propensity of poisoning. We recently hypothesized that the core-shell nanoparticles (CSNs) could be used to solve some of these problems. Part of the concept is related to the high stability and the reactivity of CSNs by which they can be assembled in a controllable way. While the use of surface protected nanoparticles as catalysts has the effect of preventing particles from aggregation, catalytic activity may become hindered due to possible inhibiting surface

materials. To demonstrate the viability of the CSN based catalysis, we recently explored pathways that take advantage of the CSNs solubilities and functionalities to assemble thin films, and the controllable activation by core-shell surface re-constitution. The formation of surface oxygenated species is found to play an important role in the effective catalytic abilities of such thin film catalysts. In this paper, our latest results of an investigation of issues related to the catalytic activation are described.

EXPERIMENT

Synthesis. The 2-nm gold nanoparticles ($Au_{2\text{-nm}}$), and 2.5 nm Au/Pt nanoparticles ($(Au/Pt)_{2.5\text{-nm}}$), were encapsulated with alkanethiolate monolayer shells were synthesized by the standard two-phase method [10]. Briefly, $AuCl_4^-$, or $AuCl_4^-$ + $PtCl_6^{2-}$ (5:1 feed ratio), was transferred to organic solvent by phase transfer agent (tetraoctylammonium chloride), and reduced by sodium borohydride in the presence of decanethiols (DT). The reaction was allowed to proceed under stirring at room temperature for 4 hours, producing a dark-brown solution of DT-encapsulated nanoparticles that was then cleaned in ethanol or used in the heating treatment.

Processing. Highly-monodispersed Au particles (5.3 ±0.3 nm) were prepared by thermally activated treatment of the pre-synthesized 2-nm Au nanoparticles [2]. Briefly, the 2 nm particles were pre-concentrated by a factor of ~15, heated to 140 ^{0}C, and annealed at 100 ^{0}C for ~2 hours. The resulting red nanoparticle solution was then cleaned in ethanol.

Thin film Assembly. The nanoparticles were assembled as thin films on electrode surfaces using molecular linkers via one-step exchange-crosslinking-precipitation route [4]. In a typical experiment, 1,9-nonanedithiols (NDT) were mixed in a hexane solution with DT-encapsulated nanoparticles (0.1~10 μM) and NDT (0.5~5.0 mM). The film thickness was controlled by immersion time. The films were thoroughly rinsed with pure solvent before characterizations.

Pt impregnation in Conducting Polymer Matrix. Polyaniline films with Pt loading were prepared by electrochemical method as reported by Lamy and co-workers [11]. Briefly, 0.1 M aniline was dissolved in 0.5 M H_2SO_4 solution. The polyaniline film was deposited by cyclic potential sweeping between –200 and +1000 mV at 50 mV/s. Polymerization was terminated when the oxidation peak current of ~7 mA/cm^{-2} was achieved. Pt was then deposited into the film at a potential of –200 mV (vs. Ag|AgCl|Sat'd KCl) for 5 minutes in a 10^{-4} M K_2PtCl_6 solution. The activation of the film involved thermal activation at 300 ^{0}C (instead of electrochemical polarization), details of which will be reported elsewhere.

Measurements. Electrochemical measurements (EG&G Potentiostat/Galvanostat 273A) were performed in a standard 3-electrode system using Ag|AgCl|Sat'd KCl as reference electrode, Pt as counter electrode and thin film coated glassy carbon (GC) as working electrode (0.5cm^2). Cyclic voltammetry was performed for characterizing the electrooxidation of both methanol (MeOH, Aldrich) and carbon monoxide (CO, Linde Gas) in alkaline electrolyte (0.5M KOH) with scan rate 50 mV/s. Atomic Force Microscopic (AFM) images were acquired using a Nanoscope IIIa (Digital Instruments).

RESULTS AND DISCUSSION

The existence of thiolate encapsulation and NDT-linkage in the nanoparticle films has been characterized in recent publications [1-2,4]. Figure 1 shows a representative tapping-mode AFM image for a NDT-$Au_{2\text{-nm}}$ thin film assembled on GC. The particle size and distribution are relatively uniform. The assembled nanoparticles appear to be individually-isolated. The existence of nanoporosity is also evident. The particles appear somewhat larger than the core-shell particle size due to tip-sample convolution, but a cross-section view reveals an average height as expected for the particle size. Similar morphology has also been observed for NDT-$Au_{5\text{-nm}}$ film.

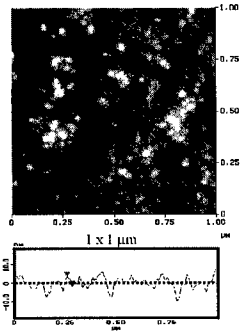

Figure 1. AFM image of NDT-linked $Au_{2\text{-nm}}$ film.

Figure 2 shows a typical set of cyclic voltammetric curves for NDT-$Au_{5\text{-nm}}$ thin film electrode in 0.5 M KOH in the presence of CO (saturated). The catalytic activity is dependent on the activation of the film. The thin film shows a featureless characteristic when it is cycled between -400 and +400 mV (A). In contrast, the film becomes catalytically active to CO oxidation when the electrode is subject to a positive polarization to ~ +700 mV. Following the large oxidation current, a large anodic wave is observed in the negative sweep (B). This wave is attributed to CO electrooxidation to CO_3^{2-} in the alkaline condition. This wave was found to be proportional to both scan rate and CO concentration [12]. The need for a positive potential polarization is believed to be associated with the participation for oxygen species near the catalytic sites at the Au nanocrystal surface. The polarization therefore likely results in the formation of gold oxide species (AuO_x) and a partial removal of the organic shell molecules. These surface species or sites may be operative in catalysis in two ways. First, they reduce the barrier nature of the shell component and increase the conductivity of the thin films. Secondly, the reconstituted shell may preserve the nanocrystal core size.

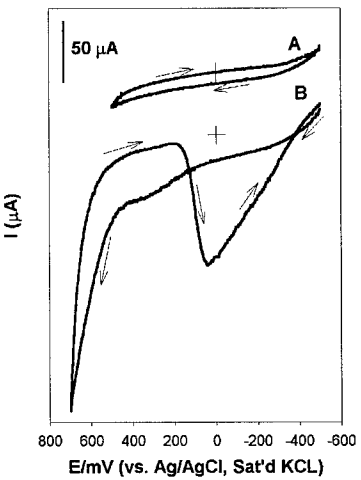

Figure 2: Cyclic Voltammograms of NDT-$Au_{5\text{-nm}}$ /GC; (a) unactivated, (b) activated. Electrolyte: 0.5 M KOH, sat'd CO, Electrode area: 0.5 cm^2 (50mv/s).

The electrocatalytic activity of the film towards methanol oxidation was examined. Figure 3 shows a representative set of CV curves for a NDT-$(Au/Pt)_{2.5\text{-nm}}$ thin film in the presence of 5 M MeOH in 0.5 M KOH. A similar effect of catalytic activation is observed. In the absence of activation (A), the voltammetric curve displays featureless characteristic. Upon

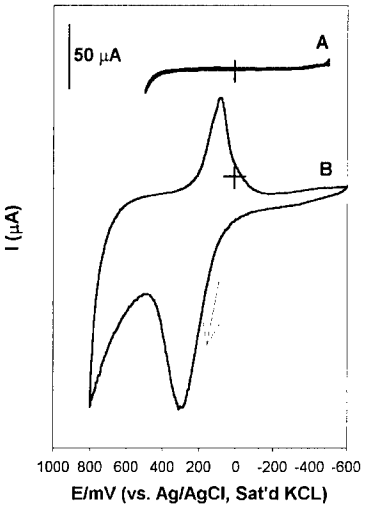

Figure 3: Cyclic Voltammograms of NDT-$(Au/Pt)_{2.5\,nm}$/GC; (a) unactivated, (b) activated. Electrolyte: 0.5 M KOH + 5.0 M MeOH, Electrode area: 0.5cm^2 (50 mv/s).

electrochemical activation of the film to a positive polarization potential (+800 mV), a large anodic wave is evident at +300 mV. The peak potential closely matches the potential for Au oxide formation, suggestive of the participation of Au oxide in the overall catalytic oxidation mechanism. An integration of the charge from the cathodic wave translates to ~$9x10^{-9}$ moles/cm^2 for the amount of reactive Au. An estimate of the catalytic peak current and the quantity of metals yields ~5 mA/mg. Through a systematic study of the concentration and scan rate dependencies, we found two remarkable voltammetric features [13]. First, the anodic peak current increases with increasing methanol concentration, exhibiting a linear relationship. Second, in contrast to the trend for the anodic wave, the peak current for the cathodic wave decreases with increasing methanol concentration, which also exhibits a linear relationship [13]. These two features form an important set of evidence demonstrating that methanol is oxidized at the nanostructured Au catalyst. The opposite trend between the oxidation and the reduction peak currents as a function of methanol concentration is suggestive of a catalytic mediation mechanism involving redox of the surface Au oxide species. Contribution from Pt oxide may be minimum because its redox potential is more positive than Au oxide and the alloyed Pt is a very small fraction (~5%). The shell encapsulation may become partially open as a result of either the surface oxide formation or a change in shell packing due to possible thiolate desorption or reorganization. The participation of surface oxide species in the above reactions is supported both by the occurrence of the oxidation wave at the potential of gold oxidation and the suppression of the gold oxide reduction wave [12,13a], and by our recent electrochemical quartz-crystal microbalance detection of mass increase in the oxidation process [13b].

It has been demonstrated that the oxidation of MeOH often involves CO as an intermediate species. The CO intermediates are often the cause of poisoning of the Pt-group catalyst. It appears that for our catalyst films the catalytic activity is relatively stable over repetitive cycling up to 50 cycles in the presence of methanol or CO. This finding is consistent with the high catalytic activity of CO oxidation observed on bare gold nanoparticles supported on oxides [8]. While a detailed investigation of the reconstituted surface species in the activation and oxidation processes is in progress, we believe that the assembled gold nanoparticles are effective catalysts for both CO and MeOH oxidation in alkaline solution. This assessment may prove extremely important as

we develop high performance fuel cell catalysts that have a long lifetime. A further assessment of possible changes of the catalyst morphology due to the activation and the formation of oxygenated species is under way with the aid of in-situ AFM technique [14].

In view of the high catalytic activity of Pt in methanol oxidation [14], we examined a different approach to incorporate Pt component in the catalytic film. In this approach, we first prepared a polyaniline thin film that was loaded with Pt. The Pt loading was accomplished via electrochemical deposition from $PtCl_6^{-2}$ anions in solution into the conductive polymer by reducing Pt^{IV} into Pt^0 particles. The NDT-$Au_{2\text{-nm}}$ film was then assembled on the surface of the polymer thin film. Figure 4 shows a preliminary set of CV data for this "layered" nanoparticle thin film in 2.5 M MeOH + 0.5 M KOH electrolyte. In the absence of activation, the voltammetric characteristic is basically silent, similar to the observation for NDT-$Au_{2\text{-nm}}$ film. Upon thermal activation, the film shows a large oxidation wave at a potential of -180 mV, much more negative than those observed earlier. We attribute the shift of the oxidation wave to the catalytic oxidation of methanol on Pt particles. While this peak potential corresponds closely to that of bulk platinum in alkaline solutions, the oxidation wave traditionally observed for the Pt catalyst on the return negative sweeping is largely absent, even after ~50 cycles. This may suggest that the traditional poisoning effect may be suppressed by the presence of gold nanoparticles. It is also possible that the intermediate CO species is oxidized by gold nanoparticles. In fact a small anodic wave is identifiable at ~+300 mV, corresponding to methanol oxidation at gold nanoparticle sites.

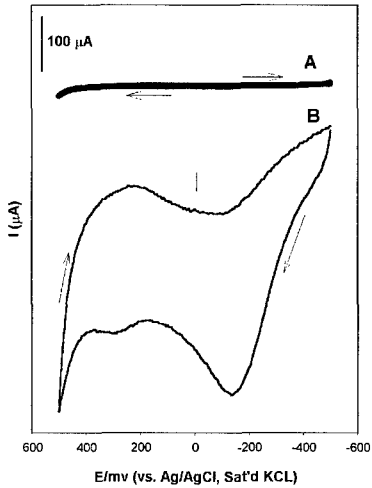

Figure 4: Cyclic Voltammograms of NDT-$Au_{2\text{-nm}}$ + PANI (Pt) thin film at a GC electrode; (a) unactivated, (b) thermally activated. Electrolyte: 2.5 M KOH + 2.5 M MeOH; Electrode area: 0.5 cm^2 (50 mv/s).

An estimate of the catalytic current vs. the quantity of metals yields ~4 mA/mg, (based on quantities of Pt and Au deposited in the film). This is qualitatively consistent with observations reported for Pt-Ru catalysts loaded in polyaniline film [11], where a ~3 mA/mg current density was found under the condition of controlled potential electrolysis. The two-component system using different approaches is another viable pathway towards the development of a poison-free catalyst.

CONCLUSION

In conclusion, the catalytic activity of the nanostructured catalyst materials was found to be tailorable by three types of interfacial chemistries. First, the utilization of functional shell of the CSNs system is important for the assembly of nanostructures that

protect particles form aggregation. The second finding for these systems reinforces the belief that the CSNs catalytic activity can be activated by activation strategies that involve reconstitution of the core-shell structure and composition. Thirdly, the Au-Pt two-component system can effectively increase the catalytic activity. The role of the organic encapsulation is important in two aspects. First, it allows controllable fine-tuning of the core size and composition via synthesis and processing. Secondly, it allows thin film assembly at any substrates. How does the shell and network encapsulation evolve and reconstitute during the catalytic activation and oxidation is a subject of our on-going investigations.

ACKNOWLEDGMENTS

Financial support of this work is gratefully acknowledged from the ACS Petroleum Research Foundation and 3M Corporation.

REFERENCES

1. M. Brust; M. Walker; D. Bethell; D. J. Schiffrin, R. Whyman, *Chem. Commun.*, 801, (1994).
2. (a) M. M. Maye; W. X. Zheng; F. L. Leibowitz; N. K. Ly; C. J. Zhong, *Langmuir*, , **16**, 490, (2000) (b) M. M. Maye; C. J. Zhong, *J. Mater. Chem.*, **10**, 1895, (2000).
3. (a) D. Bethell, M. Brust, D.J. Schiffrin, C. Kiely, *J. Electroanal. Chem.* **409**, 137, (1996). (b) J.K.N. Mbindyo; B.D. Reiss; B.R. Martin; C.D. Keating; M.J. Natan; T.E. Mallouk, *Adv. Mater.*, **13**, 249. (2001).
4. F. L. Leibowitz; W. X. Zheng; M. M. Maye; C. J. Zhong, *Anal. Chem.*, **71**, 5076, (1999).
5. A. C. Templeton; W. P. Wuelfing, R. W. Murray; *Acc. Chem. Res.* **33,** 27; (2000) and references therein.
6. F. Caruso, *Adv. Mater*, **13**, 11; (2001), and references therein.
7. (a) J. J. Storhoff; C. Mirkin, *Chem. Rev.* , **99** , 1849, (1999). (b) S. Mann; W. Shenton; M. Li; S. Connolly; D. Fitzmaurice, *Adv. Mater.*,**12**, 147 (2000).
8. (a) M. Haruta, *Catalysis Today*, , **36**, 153. (1997) (b) P. C. Biswas; Y. Nodasaka; M. Enyo; M. Haruta, *J. Electroanal. Chem.*, **381**, 167, (1995).
9. (a) G. C. Bond and D. T. Thompson, *Catal. Rev.*,**41,** 319 (1999). (b) G. C. Bond, D. T. Thompson, *Gold Bulletin*, **33**, 41 (2000).
10. (a) M. J. Hostetler; J. E. Wingate; C. J. Zhong; J. E. Harris; R. W. Vachet; M. R. Clark; J. D. Londono; S. J. Green; J. J. Stokes; G. D. Wignall; G. L. Glish; M. D. Porter; N.D. Evans; R. W. Murray, *Langmuir*, ***14***, 17. (1998).
11. A. Lima, C. Coutanceau, J.-M. Leger, C. Lamy; *J. Appl. Electrochem.*, **31**, 379, (2001)
12. M. M. Maye; Y. Lou; C. J. Zhong, *Langmuir*, **16**, 7520. (2000).
13. (a) Y. Lou; M. M. Maye; L. Han; J. Luo; C. J. Zhong, *Chem. Comm.*, 473, (2001). (b) J. Luo; Y. Lou; M. M. Maye; C. J. Zhong; M. Hepel, *Electrochemistry Communications*, , **3**, 172. (2001).
14. M. M. Maye, J. Luo, L. Han, C.J. Zhong; *Nano Letts.*, **1**,10, 575, (2001).